Report on a problem studied at the UK Mathematics-in-Medicine Study Group Nottingham 2000
< http://www.maths-in-medicine.org/uk/2000/drug-delivery/ >

Drug delivery by magnetic microspheres

Giles Richardson, Linda Cummings, John King, Nottingham;
Eamonn Gaffney, Birmingham;
Lee Hazelwood, Southampton;
Jon Chapman, Oxford.

February 2001

1 Introduction

Magnetically targeted drug delivery is a method for delivering a drug to a specific site in the body. It is made possible by attaching the drug to small paramagnetic particles. These are then injected into the patient's blood stream and are attracted to the target (for example a tumour) by inducing a magnetic field which has a maximum intensity close to the target. The advantages of this method over conventional drug delivery are that much smaller doses of the drug (which in many cases are highly toxic) are required to treat the patient and larger concentrations can be achieved at the target site. In practice the magnetic field is usually generated by placing a magnet on the surface of the patient as close to the target site as possible.

In order to investigate this process we will formulate a model based on a setup which is schematically represented in figure 1. We consider a blood vessel in the target region, inside which magnetic microspheres are being convected. Typically the radius of the microspheres, a, is much smaller than the width of the blood vessel, h. This in turn is typically much smaller than the lengthscale of the magnet, L. The distance of the magnet away from the target region is usually comparable with the lengthscale of the magnet (i.e. $O(L)$).

We begin by outlining the physics underlying the process, in §2. In §3 we formulate a general mathematical model intended to describe this process for a single magnetic particle, firstly in three space dimensions, before restricting to two dimensions in §3.1 for some explicit calculations. In §4 we list some possible extensions to the model and summarise its limitations, notable among these being the omission of interaction between particles. We conclude in §5 by using force and energy estimates to investigate the possible effects of particle-particle interaction, and the formation of 'chains' of particles under the influence of the magnetic field.

2 The Physics

The forces acting on an isolated particle are:

1. A magnetic force $\boldsymbol{F}_m$ which for a paramagnetic particle is given by

$$\boldsymbol{F}_m = \frac{\Upsilon \mathrm{Vol}}{2\mu_0} \nabla(|\boldsymbol{B}|^2). \tag{1}$$

   Here Vol is the volume of the particle, μ_0 is the magnetic susceptibility of free space, $\boldsymbol{B}$ the magnetic field and Υ is a dimensionless number related to the magnetic susceptibility χ of the particle by the formula

$$\Upsilon = \frac{\chi}{1 + \mathcal{E}\chi},$$

   where $\mathcal{E}$ is a shape constant, see for example [6]. It takes values 0 for a needle and 1/3 for a solid sphere. The susceptibility $\chi \gg 1$ always, so if we have a solid spherical particle, $\Upsilon \approx 3$. For elongated particles however, Υ can be large.

2. The Stokes drag $\boldsymbol{F}_s$. Where we assume that the particle is spherical and has radius a very much smaller than the width of the blood vessel h, the drag on the particle when it lies many radii away from the edge of the vessel can be accurately approximated by the Stokes law for drag on a particle in an infinite medium,

$$\boldsymbol{F}_s = -6\pi\mu a(\boldsymbol{V} - \boldsymbol{u}). \tag{2}$$

   Here μ is the viscosity of the fluid in the vessel, $\boldsymbol{V}$ is the velocity of the particle and $\boldsymbol{u}$ is the velocity of the fluid. For large enough blood vessels it is reasonable to assume that the flow in the vessel is Poiseuille flow. For smaller vessels with diameter comparable to the width of a red blood cell this assumption breaks down.

3. Gravitational force. In all situations of interest this is negligible in comparison with the other forces.

4. Magnetic interactions between particles. We ignore these in our model formulation of §3, though we discuss their possible effect in §5. Such interactions may lead to clustering of particles, and subsequent blockage of smaller blood vessels.

In addition to these forces the particle moves in response to random thermal excitations (Brownian motion). A measure of the importance of this effect [2] is given by consideration of the rate of change of the mean square of the distance r of the particle from its starting position in a quiescent fluid

$$\frac{d\langle r^2 \rangle}{dt} = \frac{6kT}{Q} = \frac{kT}{\pi\mu a}.$$

Here T is the absolute temperature of the fluid, k is Boltzmann's constant and Q is the drag coefficient of the particle, in other words, the constant of proportionality relating the force on the particle to its velocity. In this case Q is obtained from equation (2). The above formula can be used to calculate the diffusion coefficient α of a number of particles; here we find $\alpha = kT/(6\pi\mu a)$.

Typical measurements for: a, the radius of the particle, h, the width of the blood vessel, L, the lengthscale of the magnet, $|\boldsymbol{B}|$, the magnitude of the magnetic field, ρ, the density of the particle, U, the velocity of the blood flow in the vessel, μ, the viscosity of the blood, k, Boltzmann's constant, Υ the shape dependant magnetic susceptibility of the particle, T, the temperature and μ_0, the magnetic susceptibility of free space are given below.

$$a \sim 10^{-8} - 10^{-6} \ \text{m}, \qquad h \sim 10^{-5} - 10^{-3} \ \text{m}, \qquad L \sim 10^{-2} \ \text{m}$$

$$|\boldsymbol{B}| \sim 10^{-4} - 1 \ \text{N Amp}^{-1}\,\text{m}^{-1}, \qquad \rho \sim 10^{3} - 10^{4} \ \text{kg m}^{-3}, \qquad U_0 \sim 10^{-3} - 10^{-1} \ \text{m s}^{-1},$$

$$\mu \sim 10^{-3} \ \text{kg m}^{-1}\text{s}^{-1}, \qquad k = 1.381 \times 10^{-23} \ \text{N m Kelvin}^{-1}, \qquad \Upsilon \sim 3,$$

$$T \sim 310 Kelvin \qquad \mu_0 = 4\pi \times 10^{-7} \ \text{Amp}^{-2}\text{N}$$

3 Formulation of a model

Motion of the particle in the blood flow

We start by considering the motion of a single magnetic particle in the blood flow so that no magnetic or fluid dynamical complications arise due to interactions with other particles. We shall assume that the vessel is cylindrical with arbitrary cross-section Ω and with axis lying parallel to the x-axis. Furthermore we assume the flow is Poiseuille such that the fluid velocity

$$\boldsymbol{u} = U(y,z)\boldsymbol{e}_x,$$

and that the diffusional effect of thermal fluctuations is negligible. In practice this last assumption is reasonable for larger blood vessels but would not be reasonable for smaller vessels containing small microspheres. For example, if we take microspheres of the order of 10^{-8} m the timescale for significant diffusion of these across a vessel of size 10^{-5}m is of the order of one second.

If the position of the particle is given by $(x,y,z) = (X(t), Y(t), Z(t))$, and $B = |\boldsymbol{B}|$, the equations of motion of the particle are, on neglecting diffusional effects,

$$\rho\left(\frac{4\pi a^3}{3}\right)\frac{d^2X}{dt^2} = \frac{\Upsilon}{\mu_0}\left(\frac{4\pi a^3}{3}\right)B\frac{\partial B}{\partial x} + 6\pi\mu a\left(U(Y,Z) - \frac{dX}{dt}\right), \tag{3}$$

$$\rho\left(\frac{4\pi a^3}{3}\right)\frac{d^2Y}{dt^2} = \frac{\Upsilon}{\mu_0}\left(\frac{4\pi a^3}{3}\right)B\frac{\partial B}{\partial y} - 6\pi\mu a\frac{dY}{dt}, \tag{4}$$

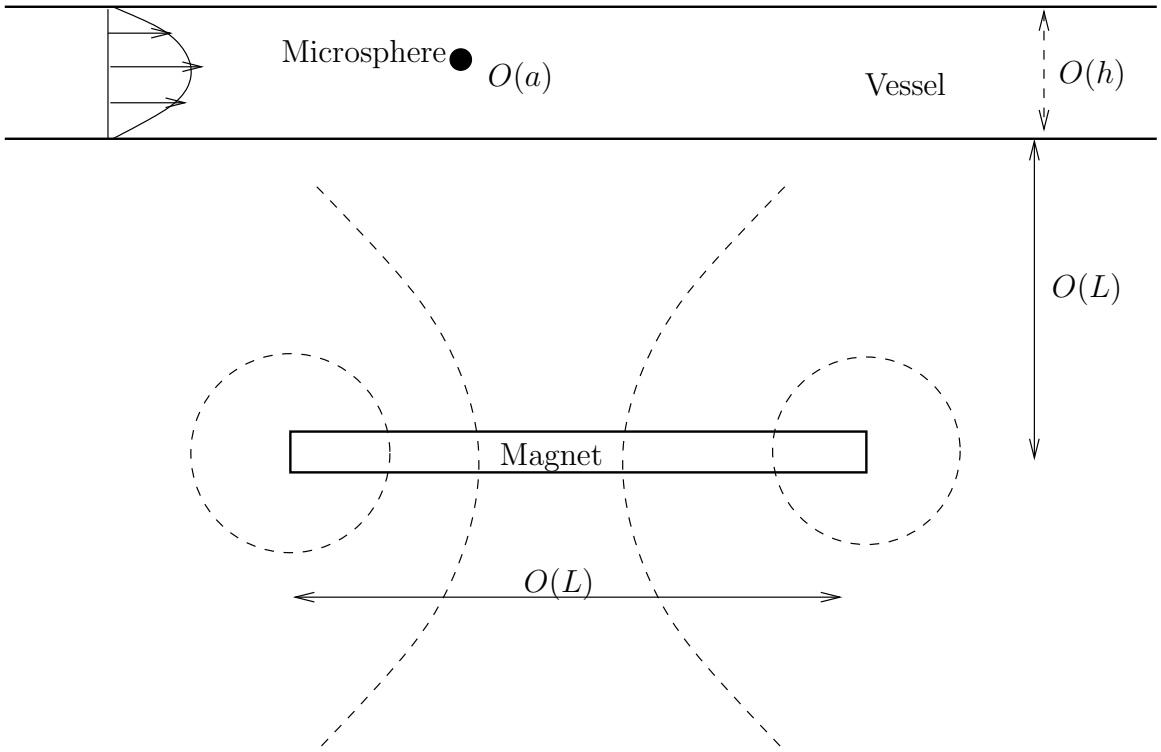

Figure 1: The model

$$\rho\left(\frac{4\pi a^3}{3}\right)\frac{d^2Z}{dt^2} = \frac{\Upsilon}{\mu_0}\left(\frac{4\pi a^3}{3}\right)B\frac{\partial B}{\partial z} - 6\pi\mu a\frac{dZ}{dt}. \tag{5}$$

We then non-dimensionalise these equations as follows:

$$\left.\begin{aligned} &x = L\hat{x}, \quad y = L\hat{y}, \quad z = L\hat{z}, \quad B = B_0\hat{B}, \\ &X = L\xi, \quad Y = h\eta, \quad Z = h\nu, \quad t = \frac{L}{U_0}\hat{t} \\ &U = U_0\hat{U}. \end{aligned}\right\} \tag{6}$$

This gives the following dimensionless system:

$$N\frac{d^2\xi}{d\hat{t}^2} = M\delta\left(\hat{B}\frac{\partial\hat{B}}{\partial\hat{x}}\right)\Bigg|_{\substack{\hat{x}=\xi \\ \hat{y}=\delta\eta \\ \hat{z}=\delta\nu}} + \left(\hat{U}(\eta,\nu) - \frac{d\xi}{d\hat{t}}\right), \tag{7}$$

$$N\frac{d^2\eta}{d\hat{t}^2} = M\left(\hat{B}\frac{\partial\hat{B}}{\partial\hat{y}}\right)\Bigg|_{\substack{\hat{x}=\xi \\ \hat{y}=\delta\eta \\ \hat{z}=\delta\nu}} - \frac{d\eta}{d\hat{t}}, \tag{8}$$

$$N\frac{d^2\nu}{d\hat{t}^2} = M\left(\hat{B}\frac{\partial\hat{B}}{\partial\hat{y}}\right)\Bigg|_{\substack{\hat{x}=\xi \\ \hat{y}=\delta\eta \\ \hat{z}=\delta\nu}} - \frac{d\nu}{d\hat{t}}, \tag{9}$$

where the dimensionless parameters N, M and δ are defined by

$$M = \frac{2\Upsilon a^2 B_0^2}{9\mu_0 U_0 \mu h}, \quad N = \frac{2\rho a^2 U_0}{9\mu L}, \quad \delta = \frac{h}{L}.$$

In all cases of interest $N \ll 1$ and hence we can neglect inertia terms in (7)-(9). Where $M \ll 1$ equations (8) and (9) imply that the particle hardly changes its position in the flow as it passes the magnet. If $M \gg 1$ then it can be inferred from these equations that the particle is strongly attracted to the wall and will certainly reach it before being convected past the magnet. The situation of greatest interest is thus $M = O(1)$, and in this scenario we can neglect the first term on the right-hand side of (7) since $\delta \ll 1$. We can further simplify equations (7)–(9), using the small size of δ, by evaluating the quantities involving the magnetic field on $\hat{y} = 0$, $\hat{z} = 0$; this yields

$$\frac{d\xi}{d\hat{t}} \sim M\delta\left(\hat{B}\frac{\partial\hat{B}}{\partial\hat{x}}\right)\Bigg|_{\substack{\hat{x}=\xi \\ \hat{y}=0 \\ \hat{z}=0}} + \hat{U}(\eta,\nu), \tag{10}$$

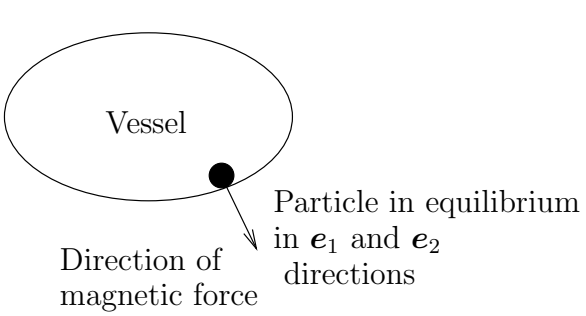

Figure 2: A picture showing the equilibrium position of the particle in the plane normal to the axis of the vessel.

$$\frac{d\eta}{d\hat{t}} \sim M\left(\hat{B}\frac{\partial \hat{B}}{\partial \hat{y}}\right)\Bigg|_{\substack{\hat{x}=\xi \\ \hat{y}=0 \\ \hat{z}=0}}, \qquad \frac{d\nu}{d\hat{t}} \sim M\left(\hat{B}\frac{\partial \hat{B}}{\partial \hat{y}}\right)\Bigg|_{\substack{\hat{x}=\xi \\ \hat{y}=0 \\ \hat{z}=0}}. \tag{11}$$

The particle on the wall of the vessel

As a result of the particle's motion under the action of the magnetic field it may eventually come very close to the wall. In this regime the assumptions about the particle moving in an effectively infinite medium break down and hence the Stokes law (2) also. However, following Goldman, Cox and Brenner [3], we can write down the following drag law in the x-direction

$$(\boldsymbol{F}_s \cdot \boldsymbol{e}_x) = -6\pi\mu a K_f \left(0.269\dot{X}\log\left(\frac{a}{\gamma}\right) - a\left.\frac{\partial U}{\partial n}\right|_{\partial\Omega}\right) \qquad \gamma \ll a. \tag{12}$$

Here γ is the shortest distance between the particle and the wall, $\partial U/\partial n$ is evaluated at this point on the wall, and $K_f = 1.858$. Although γ is unknown, it is well known that it is always strictly positive. Hence we can equate the drag with the magnetic force on the particle in the x-direction to find its equilibria and determine their stability.

We have implicitly assumed that the particle remains very close to the wall such that $\gamma \ll a$. This is only a valid assumption where the diffusion coefficient of the particles (caused by thermal excitations) is much smaller than the radius of the particle. In practice this is hardly ever the case and the model consequently needs further refinement before it can be expected to give quantitative results.

A Stokes drag law analogous to (12) can be found in the other direction tangential to the plane of the vessel wall (perpendicular to x). It is, however, unnecessary to write this down since the particle reaches an equilibrium position on the side of the vessel in the $\boldsymbol{e}_y$ and $\boldsymbol{e}_z$ directions much more quickly than it travels a significant (i.e $O(L)$) length down the vessel, simply because the lengthscale in the $\boldsymbol{e}_y$ and $\boldsymbol{e}_z$ directions is much smaller than L (the lengthscale in the $\boldsymbol{e}_x$ direction). We can therefore make the assumption that as soon

as the particle makes contact with the side wall it moves to its equilibrium position on the wall (see figure 2).

Equating $\boldsymbol{F}_s \cdot \boldsymbol{e}_x$, as given by (12), and the magnetic force $\boldsymbol{F}_m \cdot \boldsymbol{e}_x$, given by (1), we find

$$\frac{\Upsilon}{\mu_0}\left(\frac{4\pi a^3}{3}\right) B\frac{\partial B}{\partial x} = 6\pi\mu a K_f \left(0.269\dot{X}\log\left(\frac{a}{\gamma}\right) - a\left.\frac{\partial U}{\partial n}\right|_{\partial\Omega}\right). \tag{13}$$

In terms of the dimensionless variables defined by (6) it is helpful to define the following function

$$E(\hat{x}) = \hat{B}\frac{\partial \hat{B}}{\partial \hat{x}} + \frac{\epsilon K_f}{\delta M}\frac{\partial \hat{U}}{\partial \hat{n}} \tag{14}$$

where the dimensionless parameter $\epsilon = a/h \ll 1$. The particle is in equilibrium at a point $\hat{x} = \hat{x}_{1,c}$ if $E(\hat{x}_{1,c}) = 0$. Furthermore the stability of this equilibrium can be worked out by noting that $d\xi/d\hat{t} > 0$ if $E(\hat{x}) > 0$, and $d\xi/d\hat{t} < 0$ if $E(\hat{x}) < 0$. So, an equilibrium where E changes from negative to positive as $\hat{x}$ increases is unstable, whereas one where it changes from positive to negative is stable.

3.1 The two-dimensional model

In order to make further progress we now consider a simplified two-dimensional model in which the blood vessel is replaced by a channel between two parallel planes separated by distance h and with normals along $\boldsymbol{e}_y$. For this purpose we find it convenient to take the channel as $0 < y < h$. The magnetic field is provided by a thin plate magnet which lies parallel to the channel, a distance dL away. The magnetic plate has length $2L$ in the $\boldsymbol{e}_x$ direction and is infinite in the z-direction (see figure 3). We assume that the plate has constant magnetisation per unit area, such that the magnetic field it generates is of the form

$$\boldsymbol{B} = B_0 L\nabla\left(\arctan\left(\frac{y+dL}{x-L}\right) - \arctan\left(\frac{y+dL}{x-L}\right)\right).$$

The Poiseuille fluid velocity between the sides of the channel at $y = 0$ and $y = h$ is given by

$$\boldsymbol{u} = \frac{6U_0}{h} y\left(1 - \frac{y}{h}\right)\boldsymbol{e}_x, \tag{15}$$

where U_0 is the average flow velocity in the channel.

In terms of the non-dimensional variables defined by (6) the magnitude of the magnetic field $\hat{B}$ is given by the expression

$$\hat{B}^2 = |\hat{\boldsymbol{B}}|^2 = \frac{4}{\left((\hat{x}+1)^2 + (\hat{y}+d)^2\right)\left((\hat{x}-1)^2 + (\hat{y}+d)^2\right)},$$

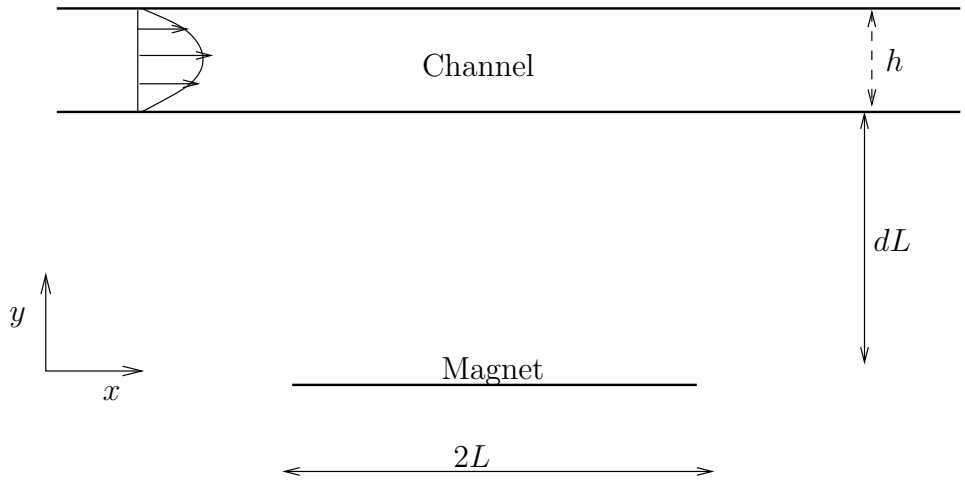

Figure 3: The two-dimensional setup.

and the flow speed $\hat{U}$ acting on a particle at position (ξ, η) is

$$\hat{U}(\xi, \eta) = 6\eta(1 - \eta).$$

Substituting these forms for the magnetic field and flow into (10) and (11) we find

$$\frac{d\xi}{d\hat{t}} = M\delta \frac{8\xi\left(1 - (\xi^2 + d^2)\right)}{\left((\xi+1)^2 + d^2\right)^2 \left((\xi-1)^2 + d^2\right)^2} + 6\eta(1-\eta), \tag{16}$$

$$\frac{d\eta}{d\hat{t}} = -M \frac{8d\left(1 + (\xi^2 + d^2)\right)}{\left((\xi+1)^2 + d^2\right)^2 \left((\xi-1)^2 + d^2\right)^2}. \tag{17}$$

We can work out the equilibrium positions of the particle on the lower boundary of the channel from the equilibrium function defined in (14), which becomes

$$E(\hat{x}) = \frac{8\hat{x}\left(1 - (\hat{x}^2 + d^2)\right)}{\left((\hat{x}+1)^2 + d^2\right)^2 \left((\hat{x}-1)^2 + d^2\right)^2} + 6\frac{\epsilon K_f}{\delta M}. \tag{18}$$

The zeros of this function give the possible equilibria.

3.1.1 Calculations based on this model

Phase trajectories of particles starting at different heights of the channel at $\xi = -\infty$ are calculated using equations (16) and (17). We take $M = 0.1$ and since $\delta \ll 1$ we neglect the first term on the right-hand side of (16). The results are plotted in figure 4 for different values of d. It can be seen that for higher values of d some of the particles fail to reach the lower surface, but for values of d less than about 1 all the particles reach the bottom surface.

We then consider the equilibria of the particle on the lower surface of the channel. We find these by plotting the first term of expression (18) as a function of $\hat{x}$. The equilibria may

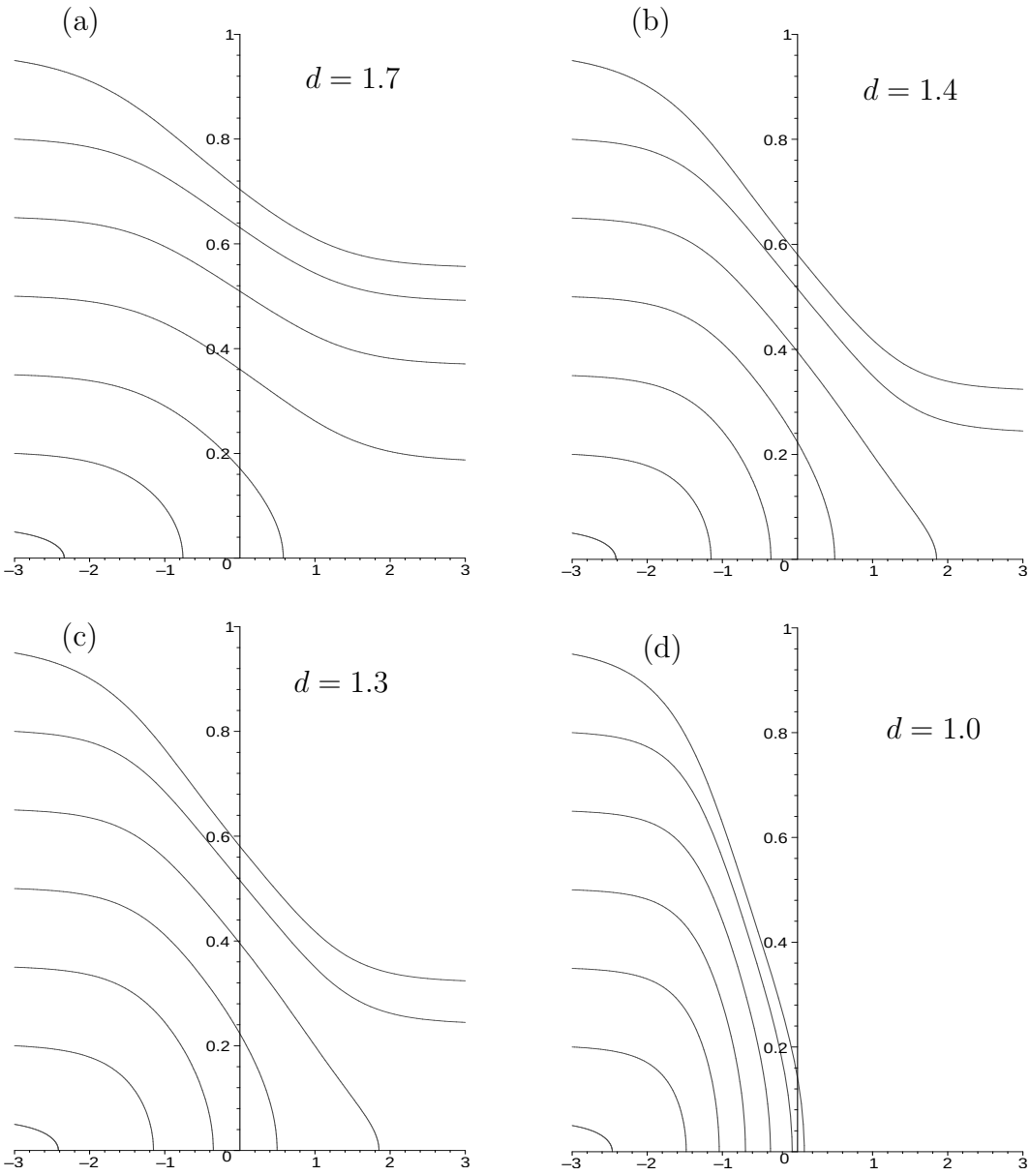

Figure 4: Phase portraits for particles moving past the magnet as the magnet channel separation, d, is varied. Here $M = 0.1$.

then be found by drawing the line $y = -6\epsilon K_f/(\delta M)$ and reading off the points at which the two curves intersect. We take $6\epsilon K_f/(\delta M) = 0.1$ and plot these two curves for various values of d. It is notable that for relatively large values of d only one stable equilibrium is possible, but for values of d less than about 0.9 two stable equilibria appear close to the edges of the magnet at $\hat{x} = -1$ and $\hat{x} = 1$.

The equilibrium which occurs for the highest value of $\hat{x}$, say $\hat{x} = \hat{x}_m$, is unstable, and, any particle which reaches the bottom surface of the channel before this equilibrium will be captured, while any particle which reaches it after this point will be swept down stream. We can thus estimate the percentage capture of particles, assuming that they are evenly distributed in the channel at $\xi = -\infty$. We do this by tracing the particle trajectory which reaches the lower surface at $\xi = \hat{x}_m$ back to $\xi = -\infty$. So, for instance, if we have $d = 1.3$, $M = 0.1$ and $6\epsilon K_f/(\delta M) = 0.1$ the highest equilibrium is $\hat{x} = \hat{x}_m = 1.92$ (figure 5b) and if we trace back the particle trajectory which reaches $(\xi, \eta) = (1.92, 0)$ to $\xi = -\infty$ we find that $\eta = 0.81$ and hence that there is 81% capture of particles in this scenario.

4 Further work

In this section we briefly outline limitations of and possible refinements to the model formulated above.

1. The effects of diffusion (caused by thermal excitations) has been neglected throughout the model. This is almost certainly an invalid assumption when we treat the case of the particle lying in close proximity to the wall of the vessel. Boltzmann's law says that, in thermodynamic equilibrium, the probability p of finding the particle at a given height h above the vessel wall is given by $p \propto \exp(-\Phi(h)/(kT))$, where Φ is the potential energy of the particle. Thus for the case we are considering

$$p \propto \exp\left(\frac{4\pi a^3 \Upsilon B \frac{\partial B}{\partial y} h}{3\mu_0 kT}\right),$$

where B and its derivatives are evaluated on the vessel wall. A measure of the length-scale for the decay of this probability is given by R where

$$R = \frac{3L\mu_0 kT}{4\pi a^3 \Upsilon B_0^2}.$$

Where $R \ll a$ the existing model is fine; but otherwise the model for the motion of the particle along the wall needs altering. If $R \geq O(h)$ a diffusive term must be included in the description of the motion of the particle in the fluid filling the vessel. A model for the capture of permanently magnetised microparticles, including the effect of their Brownian motion, has been developed by Zarutskaya and Shapiro [9]. They consider a single particle moving in a half-space filled with air and assume it is captured once it hits the lower plate.

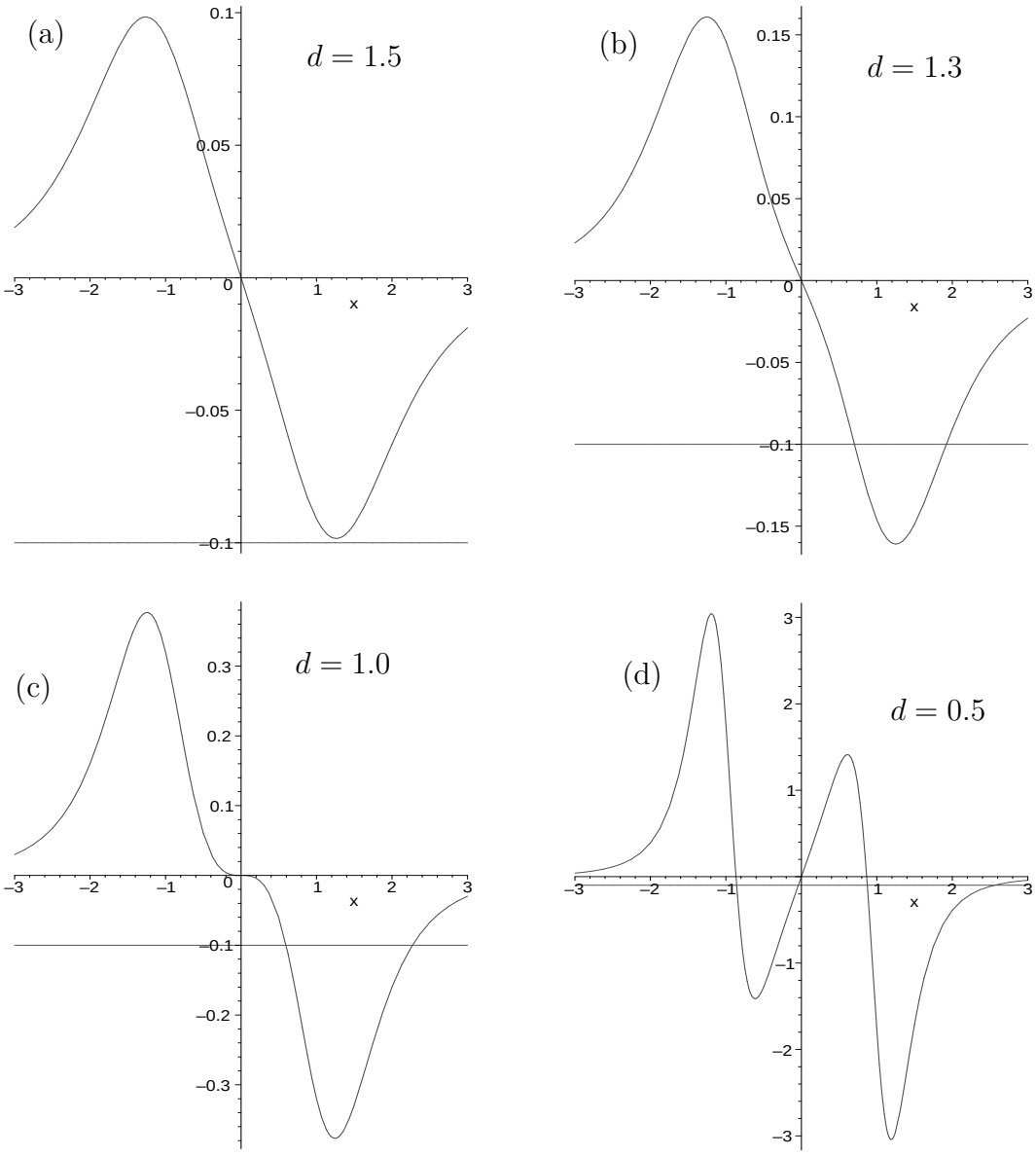

Figure 5: The intersection of the curve $y = \hat{B}\partial\hat{B}/\partial\hat{x}$ and the line $y = -0.1$ gives the equilibrium positions of a particle on the lower surface of the channel, for various values of d, and for $6\epsilon K_f/(\delta M) = 0.1$. For $d = 1.5$ there are no equilibria; for $d = 1.3$ there two are equilibria at $\hat{x} = 0.70$ and $\hat{x} = 1.92$ (stable, unstable respectively); for $d = 1.0$ there two equilibria at $\hat{x} = 0.60$ and $\hat{x} = 2.27$ (stable, unstable respectively); for $d = 0.5$ there are four equilibria at $\hat{x} = -0.86$, $\hat{x} = -0.04$, $\hat{x} = 0.87$ and $\hat{x} = 2.55$ (stable, unstable, stable, unstable respectively).

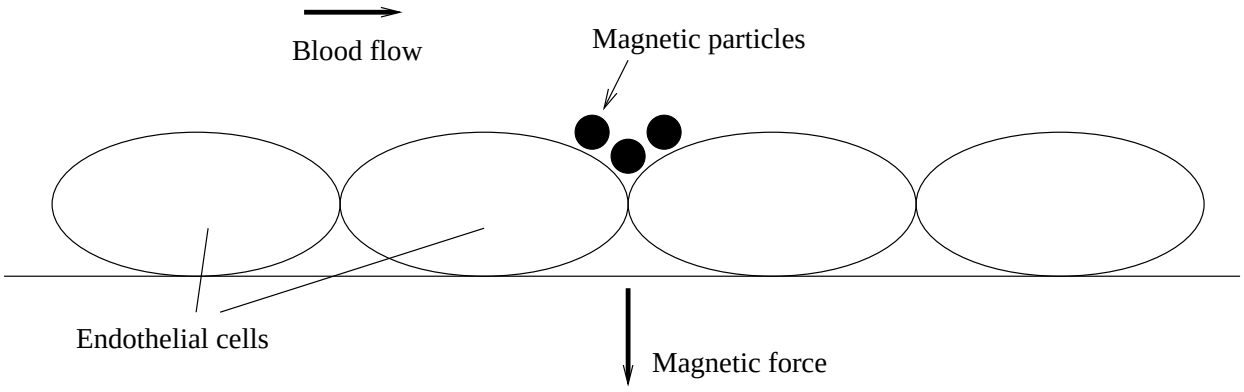

Figure 6: The vessel wall geometry.

2. In Section 3.1 we used the model to describe the transport of particles in a two-dimensional channel to which a magnetic field is applied by a two-dimensional magnet. While the analysis for this scenario is fairly simple it is not of direct relevance for the description of drug transport in capillaries. With this in mind it would be useful to formulate the model for a cylindrical vessel (which might be thought of approximating the capillary) and a disc magnet which is the commonly used method of applying the magnetic field.

3. The model could be extended with relative ease to cover cases where the magnetic drug carriers have a permanent magnetic moment. Permanently magnetised particles are briefly discussed below in §5.

4. An important practical point to determine is whether the particles become embedded in the side of the blood vessel so that when the magnetic field is removed they remain there, rather than being convected away by the blood flow. In order to address this problem knowledge of the composition of the vessel wall is required. It can then be incorporated into the model. We have assumed a smooth vessel wall which is an obvious simplification; real blood vessels are lined with endothelial cells, which are much larger than the magnetic microspheres (see figure 6). Leaving aside the complications of the altered flow field caused by this geometry at the wall, we might expect that the particles would accumulate in inter-cell'valleys' near the stable equilibria. one idea proposed, which we have not yet investigated, is that a magnetic field oscillating slowly in the x-direction may help the particles 'burrow down' between the endothelial cells, so that they remained trapped once the field is removed.

5. The assumption of a single particle in the flow is an obvious simplification, as in reality there are many particles which will interact in a very complex way, both in terms of the flow and the magnetic field. For example, even in an ordinary two-particle system with no magnetic field, the hydrodynamic drag they experience is

dependent upon their shape; the distance between them; their individual orientation; their relative orientation; the properties of the fluid; and their velocities and spins relative to the fluid. Moreover, these forces can sometimes act to tear the particles apart, and sometimes to draw them together. Detailed calculations such as these are beyond the scope of this report (see for instance [5, 7]); however we conclude the report with some elementary considerations of particle attraction and interaction in §5 below.

5 Particle chaining

We have so far assumed a single particle system throughout, which is fine as long as the particles remain well-separated in the flow. However, the applied magnetic field means that the particles are attracted to points of high intensity, and they may be brought into close proximity. When this happens they may interact, both magnetically and hydrodynamically, and some of our model assumptions may then be invalid. Clustering of particles is an issue of practical importance, as it could potentially lead to blockage of small blood vessels. This is not always undesirable; it has been suggested that this behaviour may be a useful mechanism for starving tumours [8].

Magnetic colloids suspended within fluids have been seen to exhibit interesting aggregation or chaining behaviour. The physics behind chain formation involves a competition between the magnetic, thermal and flow forces which attempt to form/destroy the particle chains. These interactions and forces are discussed in §5.1 before discussing some idealised models which estimate parameter regimes whereby particle chaining can occur in §5.2.

5.1 Particulate interactions and forces

Magnetic interactions

If one approximates the spheres by point magnetic dipoles located at their centres of mass then the magnetic interaction energy for aligned dipoles may be written

$$W_{12} = -\frac{\mu_0 |\boldsymbol{m}|^2}{4\pi r^3} \left[3\cos^2\theta - 1\right] \tag{19}$$

where $\boldsymbol{m}$ is the magnetic dipole moment, μ_0 is the permeability of free space, r is the distance between particle centres and θ the relative positional orientation of the dipoles as shown in figure 7.

The force between dipoles is thus

$$F = -\frac{\partial W_{12}}{\partial r} = \frac{3\mu_0 |\boldsymbol{m}|^2}{4\pi r^4} \left[3\cos^2\theta - 1\right]. \tag{20}$$

The minimum energy configuration is obtained when the spheres are in contact, $r = 2a$, where a is the sphere radius and $\theta = 0$ or π, favouring a head-tail configuration. This also

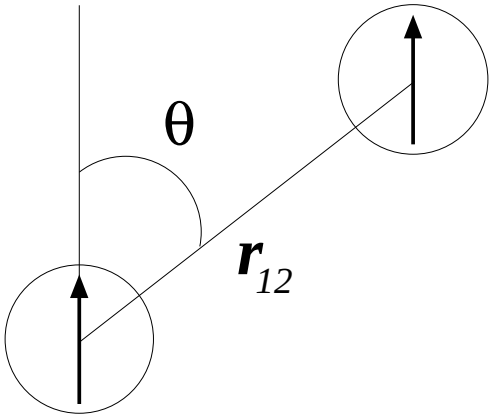

Figure 7: Point magnetic dipole-dipole construction.

corresponds to the maximum attractive force between the two dipoles. By contrast, the maximum energy configuration is obtained when $\theta = \pi/2$ or $3\pi/2$, corresponding to the greatest repulsion between dipoles. The attractive/repulsive nature of this interaction leads us to expect head-tail chaining configurations.

The magnetic moments of such particles depend on their magnetic properties. For paramagnetic materials or superparamagnetic compounds the magnetic dipole moment is induced in the direction of the applied field:

$$\boldsymbol{m} = \frac{4}{3}\pi a^3 \Upsilon \boldsymbol{H} \tag{21}$$

Equation (19) with $\theta = 0$ then gives the minimum interaction energy for two such particles as

$$W_{para} = -\frac{1}{9}\pi\mu_0 a^3 \Upsilon^2 H^2. \tag{22}$$

For permanently magnetised particles with magnetisation $\boldsymbol{M}_d$ the magnetic moment is given by

$$\boldsymbol{m} = \frac{4}{3}\pi a^3 \boldsymbol{M}_d. \tag{23}$$

A typical value of $M_d = |\boldsymbol{M}_d|$ for particles used in this application is $M_d = 4.5 \times 10^5$ Amp m^{-1}. Again the minimum interaction energy occurs in the head-tail configuration with $\theta = 0$, and according to (19) is given by

$$W_{perm} = -\frac{1}{9}\pi\mu_0 a^3 M_d^2. \tag{24}$$

Permanently magnetised particles also align their dipole moment with a magnetic field under the influence of an aligning torque given by

$$W_{torque} = -\mu_0 \boldsymbol{m} \cdot \boldsymbol{H} = \frac{4}{3}\pi\mu_0 a^3 M_d H \cos\beta, \tag{25}$$

where β is the angle between the applied field and the magnetic dipole moment.

5.2 Model chain systems

The relative orders of magnitude of the above energies determine the regimes in which chaining is likely to occur. This section considers some possible energy/force balances.

External field absent

Consider the effect of a magnetic interaction on the particles. Paramagnetic particles in a zero field possess no dipole moment and can only interact through fluid-flow-induced forces, which are not considered here. By contrast, permanently magnetised particles do interact, as they possess a magnetic dipole. If the fluid is at rest or in uniform motion then particle chaining results through a balance between the magnetic energy (24) and thermal energy $W_{therm} = kT$. The ratio of the two energies gives rise to a coupling parameter

$$\lambda_{perm/therm} = \frac{-W_{perm}}{W_{therm}} = \frac{1}{9}\frac{\pi\mu_0 a^3 M_d^2}{kT}. \tag{26}$$

One intuitively expects that thermal forces are unable to break the magnetic coupling when $\lambda_{perm/therm} > 1$. The approximate parameter values given in §2 and the typical value for the permanent magnetisation $M_d = 4.5 \times 10^5$ A m^{-1} indicate $17.06 < \lambda_{perm/therm} < 1.706 \times 10^7$, hence we expect particle chaining can occur (at least for this value of M_d).

What happens when the particles are placed in a shear flow? We have already considered the Stokes drag $\boldsymbol{F}_s$ (equation (2)) on an isolated microsphere. An estimate of the shearing force can be found by considering the difference between the forces acting on two particles located in the with centres located a distance $2a$ apart. The magnitude of this shear force in a channel of width h is of the order can be estimated using (15)

$$F_{shear} \approx 12\pi\mu a^2 \frac{\partial u}{\partial y} \sim \frac{18\pi\mu U_0 a^2}{h}, \tag{27}$$

where U_0 is the velocity in the channel. Paramagnetic particles are simply carried along by hydrodynamic forces as expected. By contrast, the permanent magnetic particles are subjected to shearing forces which attempt to disrupt the chain. Using the magnetic force (20) (with $\boldsymbol{m}$ given by (23)), together with the relative viscous force (27), yields the ratio

$$\lambda_{perm/shear} = \frac{F_{perm}}{F_{shear}} = \frac{1}{108}\mu_0 M_d^2 \frac{h}{\mu U_0}. \tag{28}$$

Note that the particle radius is absent from this expression. Only the relative magnetisation, fluid viscosity and relative fluid velocity can determine chaining structure stability. Within the parameter regime of §2 $\lambda_{perm/shear}$ is always large, and it appears unlikely that viscous shearing forces are able to destroy particle chains. With no external field the chains are simply carried along by the flow, and in principle could align themselves along the streamlines, thus minimising the shear force on the particles.

External field present

The applied magnetic field has three effects on the chain ordering: (*i*) the paramagnetic particles become magnetised along the magnetic field direction; (*ii*) the permanent magnetic particles experience torque, constraining them to lie along the field direction; and (*iii*) the particle chain is subject to a torque that tends to align the chain with the field.

Consider the effect of (*i*) in a fluid at rest or in uniform motion. As above, the stability of particle chains can be estimated by considering the ratio between the paramagnetic energy W_{para} (22) and the thermal energy $W_{therm} = kT$:

$$\lambda_{para/therm} = \frac{-W_{para}}{W_{therm}} = \frac{\pi \mu_0 a^3 \Upsilon^2 H^2}{9kT}. \tag{29}$$

Taking the applied field $H = B/\mu_0$, parameter values from §2 give a huge range of values for $\lambda_{para/therm}$ ($7.6 \times 10^{-10} < \lambda_{para/therm} < 7.6 \times 10^4$), so particle chaining is likely to occur for the larger particles at higher magnetic fields.

If these paramagnetic particles are carried in a shear flow, the coupling parameter is given by considering the ratio between the magnetic and viscous forces

$$\lambda_{para/shear} = \frac{F_{para}}{F_{shear}} = \frac{1}{108} \frac{\mu_0 \Upsilon^2 H^2 h}{\mu U_0}. \tag{30}$$

Again the particle radius is absent from this expression. Only the relative energies of magnetisation and fluid viscosity play a role in determining chaining disruption. In fact, for the parameter values of §2, $10^{-4} < \lambda_{para/shear} < 10^8$. Thus we expect that viscous forces are likely to disrupt chaining for strong flows in a narrow hannel and for small magnetic fields.

Chaining dynamics

Finally, a brief mention should be given to the actual dynamics of chaining. The rate at which chaining occurs may be an important limiting factor which may restrict the choice of physical parameters. The relative proportion of colloid to fluid, the magnetic property of the material, and the magnetic field, will all have an effect on the chaining rate. While it is obvious that colloidal percentage plays a key role, it is less obvious how the magnetic material affects chaining rate. For example, in zero field the permanent magnetic particles must approach in both positionally- and orientationally-acceptable configurations. However,

the application of a magnetic field aligns the colloidal particles with the field. Now only the positional condition must be satisfied. Thus one expects the field to increase the chaining rate for permanently magnetised particles (see [1]).

Drawbacks of the chaining model

The principal weakness of the chaining model concerns the magnetic torque that permanent magnetic particles and all magnetic chains feel on the application of a magnetic field. Including this torque within the models should yield more detailed predictions of chaining dynamics. This problem plays an extended role when the chains are placed in a shear flow. Using the techniques developed within liquid crystal and polymer physics should provide more detailed results on chaining stability.

References

[1] De Gennes, P.G., Pincus, P.A. "Pair Correlation in a Ferromagnetic Colloid". *Phys. Kondens. Materie.* **11**, 189 (1970).

[2] Feynmann R.P., Leighton R.B., Sands M. "The Feynmann Lectures on Physics, Vol. I". *Addison-Wesley* (1964).

[3] Goldman A.J., Cox R.G., Brenner H. "Slow viscous motion of a sphere parallel to a plane wall—II Couette flow". *Chem. Eng. Sci.* **22**, 653-660 (1967).

[4] Hüfeli, U. Schütt, W. Teller, J. *in* M. Zborowski (Ed.), "Scientific and clinical applications of magnetic carriers". *Plenum Press, New York* (1977).

[5] Hoppel & Brenner "Low Reynolds number hydrodynamics". *Noordhoff International publishing, Leyden.*

[6] Jin J.X., Dou S.X., Liu H.K. "Magnetic separation techniques and HTS magnets". *Supercond. Sci. Technol.* **11**, 1071 (1998).

[7] Russel, W.B., Saville, D.A., Schowalter, W.R. "Colloidal dispersions", *Cambridge* (1989).

[8] Sheng, R., Flores, G.A., Liu, J. "In vitro investigation of a novel cancer therapeutic method using embolizing properties of magnetorheological fluids". *J. Magn. Magn. Mater.* **194**, 167 (1999).

[9] Zarutskaya T., Shapiro M. "Capture of nanoparticles in magnetic filters". *J. Aerosol Sci.* **31**, 907 (2000).